Philosophical Magazine

ISSN: 1478-6435 (Print) 1478-6443 (Online) Journal homepage: http://www.tandfonline.com/loi/tphm20

First study of manganese diffusion in Cr_2O_3 polycrystals and thin films by SIMS

A. C. S. Sabioni , A. M. Huntz , L. C. Borges & F. Jomard

To cite this article: A. C. S. Sabioni , A. M. Huntz , L. C. Borges & F. Jomard (2007) First study of manganese diffusion in Cr_2O_3 polycrystals and thin films by SIMS, Philosophical Magazine, 87:12, 1921-1937, DOI: 10.1080/14786430601120462

To link to this article: http://dx.doi.org/10.1080/14786430601120462

Published online: 12 Mar 2007.

Philosophical Magazine,
Vol. 87, No. 12, 21 April 2007, 1921–1937

Taylor & Francis
Taylor & Francis Group

First study of manganese diffusion in Cr_2O_3 polycrystals and thin films by SIMS

A. C. S. SABIONI†, A. M. HUNTZ*‡, L. C. BORGES† and F. JOMARD§

†Laboratório de Difusão em Materiais/Departamento de Física/ICEB-UFOP, REDEMAT, 35400-000 – Ouro Preto, MG, Brazil
‡Laboratoire d'Etude des Matériaux Hors-Équilibre (LEMHE), CNRS ICMMO UMR 8182, Université Paris XI, 91405, Orsay, France
§Groupe d'Etude de la Matière condensée (GEMaC), CNRS UMR 8635, 92195 Meudon, France

(*Received 1 June 2006; in final form 13 November 2006*)

Chromia layers are formed on many industrial alloys and act as a protective barrier against the corrosion of the materials by limiting the diffusion of oxygen and cations. Most of these alloys contain manganese as an impurity, and manganese oxides are often found at the outer surface of the oxide films. In order to clarify the oxidation mechanism and to check if chromia acts as a barrier, manganese diffusion in chromia was studied in both polycrystals and oxide films formed by oxidation of Ni–30Cr alloy in the temperature range 700–1100°C at an oxygen pressure of 10^{-4} atm. After deposition of Mn on the chromia surface and a diffusing treatment, the manganese penetration profiles were established by secondary ion mass spectrometry. In all cases, the diffusion profiles showed two domains. For the first domain, using the solution of Fick's law for diffusion from a thick film into a semi-infinite medium, bulk diffusion coefficients were determined. For the second domain, the Le Claire model allowed the grain boundary diffusion parameter ($\alpha D_{gb}\delta$) to be obtained. Manganese diffusion does not vary significantly according to the nature and microstructure of chromia. The activation energy of grain boundary diffusion is not far from that obtained for bulk diffusion, probably on account of segregation phenomena. Manganese diffusion was compared to cationic self-diffusion and iron diffusion, and related to the protective character of chromia.

1. Introduction

Chromia films are of great importance since the protection ensured by such films against oxidizing and aggressive atmospheres is efficient for long times at temperatures as high as 1000°C. At temperatures above 1000°C a vaporization phenomenon occurs [1] which is enhanced in the presence of water vapour. However, at temperatures lower than 1000°C, chromia films are amongst the more efficient natural protectors. Thus, chromium is particularly added to stainless steels with the aim of developing a continuous chromia film rather than films of iron oxides whose growth is faster than the chromia film growth. For similar reasons, chromium is

*Corresponding author. Email: am.huntz@lemhe.u-psud.fr.

Philosophical Magazine
ISSN 1478–6435 print/ISSN 1478–6443 online © 2007 Taylor & Francis
http://www.tandf.co.uk/journals
DOI: 10.1080/14786430601120462

added to nickel-based alloys, thus coupling good mechanical properties and oxidation resistance at high temperatures. Besides, chromia films provide significant advantages in carburization conditions (coking) as the formation of a chromia scale, instead of iron or nickel oxides, induces a significant decrease of the amount of carbon deposition [2]. In nearly all these conditions, alloy base elements or alloy impurities can be incorporated in the chromia films during their growth and it is important to know the diffusion rate of various elements in such protective films. This is even more important in the case of chromia films deposited by various coating processes. The lifetime of the coating will clearly depend on the diffusion rate of the various elements through the protective film.

Having determined cationic self-diffusion [3, 4] and iron diffusion in chromia [5], the objective of this work was to study manganese diffusion in chromia since manganese is present in all stainless steels and its amount can vary from 0.2 to 1.5% depending to the steel. Moreover, it is well known that manganese oxides or $MnCr_2O_4$ spinel oxide are observed at the outer surface of chromia after oxidizing stainless steels [6]. The oxygen affinity of manganese is high and close to that of chromium, and it is still unknown why manganese oxides are found at the outer surface of chromia films.

It can be assumed that manganese atoms oxidize at the beginning of oxidation and that afterwards the chromia film grows by anionic diffusion, leaving manganese oxide on the top of the sample. However, this assumption is not satisfactory since chromia scales are known to grow by countercurrent diffusion of cation and anion, the oxygen diffusion not being far from chromium diffusion [3, 4].

Another possibility consists in the fact that chromia film appears first and simultaneously manganese atoms oxidize and diffuse rapidly through the chromia film, whereas chromia growth occurs by countercurrent diffusion of chromium and oxygen through chromia. When manganese is at the outer surface as MnO, it can react with chromia in order to give the spinel oxide. This second suggestion implies that manganese diffusion is faster than chromium diffusion through chromium oxide. In order to check this second possibility, manganese diffusion was measured in chromia polycrystals and thin films by secondary ion mass spectrometry (SIMS).

2. Experimental

2.1. *Material*

The synthetic polycrystalline chromia samples used in this work are the same as those used in previous studies for measuring Cr self-diffusion or Fe diffusion in Cr_2O_3 [3–5]. The Cr_2O_3 polycrystals were prepared by hot pressing at 1450°C, under 48 MPa, for 40 min, using high-purity powder (99.999%) supplied by Johnson Matthey Corporation. These samples have a density close to the theoretical density of Cr_2O_3, i.e. 5.21 g cm^{-3}, and a grain size of ca. 6 μm. The manganese diffusion experiments were also performed on Cr_2O_3 layers grown by oxidation of an Ni–30% Cr alloy provided by Imphy S.A., and containing some silicon (≈1.46 wt%). The NiCr samples were firstly annealed for 3 days in an Ar–H_2–H_2O atmosphere at

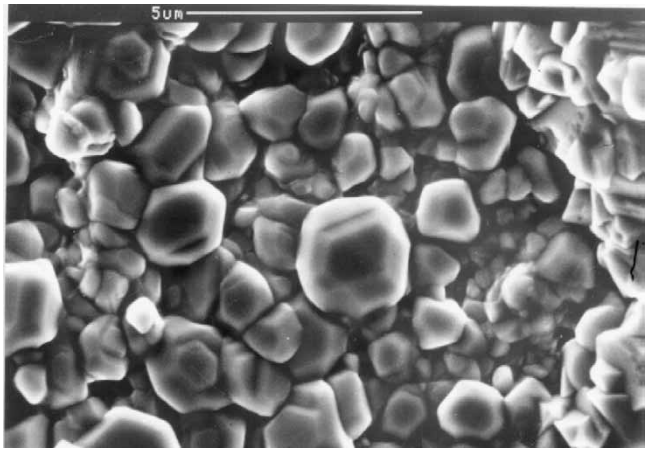

Figure 1. Microstructure (SEM) of the outer surface of the chromia film formed at 900°C on Ni–30Cr alloy.

900°C, ($pO_2 \approx 10^{-19}$ atm), in order to stabilize the grain size of the metallic substrate. Then, these samples were oxidized in laboratory air at 900°C for 112 h. It was shown previously [5] that the oxidation kinetics of such NiCr samples obey a parabolic law leading to protective compact chromia scales. At the end of this treatment, the chromia layer is about 2.5 μm thick, with an average grain size of ≈1 μm (see figure 1).

2.2. *Sample preparation*

For synthetic polycrystalline chromia, samples of 4 mm × 4 mm × 2 mm were polished in an automatic grinder/polisher Phoenix 4000/Buehler. The polishing was performed using diamond suspensions of 15, 6, 3, 1 and 0.25 μm. For chromia films, diffusion experiments were performed directly on as-oxidized samples, thus presenting a non-negligible roughness (up to 1 μm).

The samples were pre-annealed at the same oxygen pressures and temperatures to be used in the diffusion anneals. Then, an electron-beam evaporated manganese film was deposited on the polished surface using an AUTO 306 vacuum coater with a turbomolecular pumping system. High purity manganese (99.99%), supplied by Alfa Aesar (Johnson Mattey), was used in these experiments. It is worth noting that the element manganese is only composed of the isotope ^{55}Mn. It was verified that the ^{55}Mn film is about 20 nm thick, as given by the evaporating system.

2.3. *Diffusion experiments*

The manganese diffusion annealings were performed from 700 to 1100°C under a partial pressure of oxygen of 10 Pa (10^{-4} atm) obtained by using a standard mixture

of Ar/100 ppm O_2. The diffusion experiments were performed in a tubular furnace, with the sample placed in a Pt crucible inside a silica tube.

2.4. *Depth profiling by secondary ion mass spectrometry (SIMS)*

The manganese depth profiles were established by secondary ion mass spectrometry (SIMS-Cameca 4F-CNRS/Meudon/France). A 30 nm thick gold layer was deposited on the samples and a 10 keV Cs^+ primary ion source was used. The depth profiles were established by measuring the signals of the MnO^- molecular ion as a function of time (figure 2a) with some polarization of the sample support in order to filter the molecular ions except MnO^-. Indeed, in such analysis conditions, it is not possible to work with Mn^- ions due to the fact that electronic affinity of manganese is equal to zero. These experimental conditions were chosen as they allow obtaining the easiest charge compensation and the best signal stability.

The scanned area was ca. 150 μm × 150 μm and the analyzed zone was 33 μm in diameter. The depth of the craters formed on the surface of the samples after SIMS analysis was measured by means of a Talystep profilometer (KLA Tencor P1). This allowed the ion intensity of the SIMS signals to be plotted as a function of the depth in the oxide, as shown in figures 2b.

2.5. *Determination of bulk and grain-boundary diffusion coefficients*

In our experimental conditions, the iron diffusion profiles always show two distinct regions (see figure 3). Near the surface, there is a fast decrease of the concentration and, far from the surface, the concentration slowly decreases. The concentration near the surface should correspond to the contribution of the bulk diffusion, whereas the concentration far from the surface, i.e. the curve tail, should correspond to the grain-boundary diffusion [7].

2.5.1. Bulk diffusion coefficient. From the first part of the diffusion profile, a bulk diffusion coefficient was determined using an appropriate solution of the diffusion equation. In our experimental conditions, the iron film is thick in comparison with the depth of the first part of the diffusion profile. So, the diffusion coefficient (D) was determined using a solution of Fick's second law for diffusion from a thick film in a semi-infinite medium, given by [7]:

$$C(x,t) = \frac{C_o}{2}\left(\operatorname{erf}\frac{a-x}{2\sqrt{D_b t}} + \operatorname{erf}\frac{a+x}{2\sqrt{D_b t}}\right), \tag{1}$$

where C_o is the concentration at the surface, a is the thickness of the film and D_b is the bulk diffusion coefficient. The D_b values were determined by nonlinear fitting of equation (1) to the MnO^- depth profiles using the software Origin (Origin, Data analysis and Technical Graphics in Windows, version 6.0).

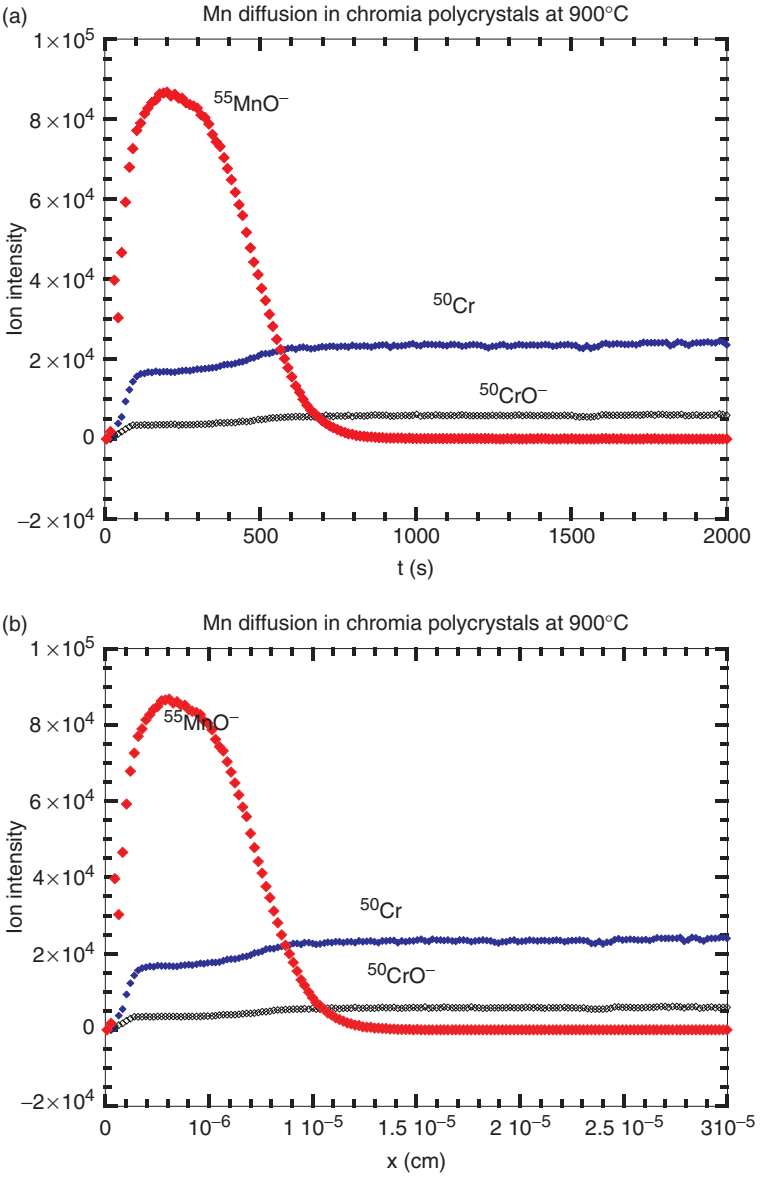

Figure 2. Penetration profile of manganese (a) vs. time and (b) vs. depth, after a diffusion treatment at 900°C for a chromia polycrystal.

2.5.2. Grain-boundary diffusion coefficient. Le Claire's model was used to determine the product $\alpha D_{gb}\delta$ from the tail of the profile by using the expression [7, 8]:

$$\alpha D_{gb}\delta = 0.661\left[-\frac{\partial(\ln C)}{\partial x^{6/5}}\right]^{-5/3}\left(\frac{4D_b}{t}\right)^{1/2} \quad (2)$$

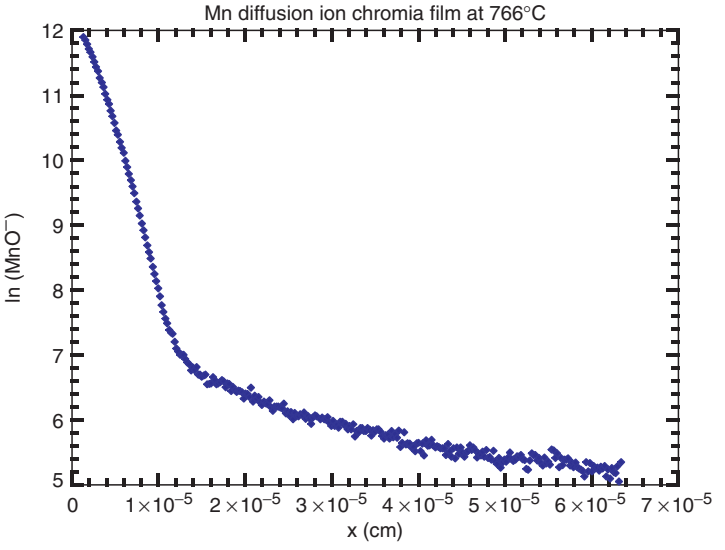

Figure 3. Penetration profile vs. the depth for MnO^- ion after a diffusion treatment at 766°C in a chromia film, showing the two parts of the profile.

where α is a dimensionless parameter known as the segregation factor [7]. The experimental points of the second part of the diffusion profiles must present a linear behaviour in a plot of $\ln C$ versus $x^{6/5}$ and the slope (γ) of the straight line in the plot of $\ln C$ versus $x^{6/5}$ (figure 4) allows the determination of the slope: $[-(\partial(\ln C))/\partial x^{6/5}]^{-5/3}$.

3. Results

Figure 5 shows the diffusion profile of MnO^- obtained in a chromia polycrystal at 900°C. The profile clearly shows two different diffusion mechanisms, as also shown in figure 3 in case of Mn diffusion in a chromia film. Similarly, the first part of the profile corresponds to bulk diffusion and the second part of the profile, i.e. the curve tail, is characteristic of the diffusion along grain-boundaries, as shown by figure 6, where the slope of the straight line corresponds to the gradient $\partial \ln C/\partial x^{6/5}$.

Similar profiles were obtained in all cases, even for the diffusion in Cr_2O_3 films, as shown in figures 7 and 8, whatever the temperature, the oxygen pressure or the nature of the oxide (polycrystal or film).

From all these profiles, according to the procedure explained in section 2.5, bulk and grain-boundary diffusion coefficients (in fact $\alpha D_{gb}\delta$) were obtained. The values are summarized in tables 1–2 with the characteristics of the test.

Figure 9 corresponds to the Arrhenius plot of the bulk and grain boundary diffusion coefficients, in polycrystals and in films, respectively. Arrhenius equations established for these different diffusion coefficients are given in table 3.

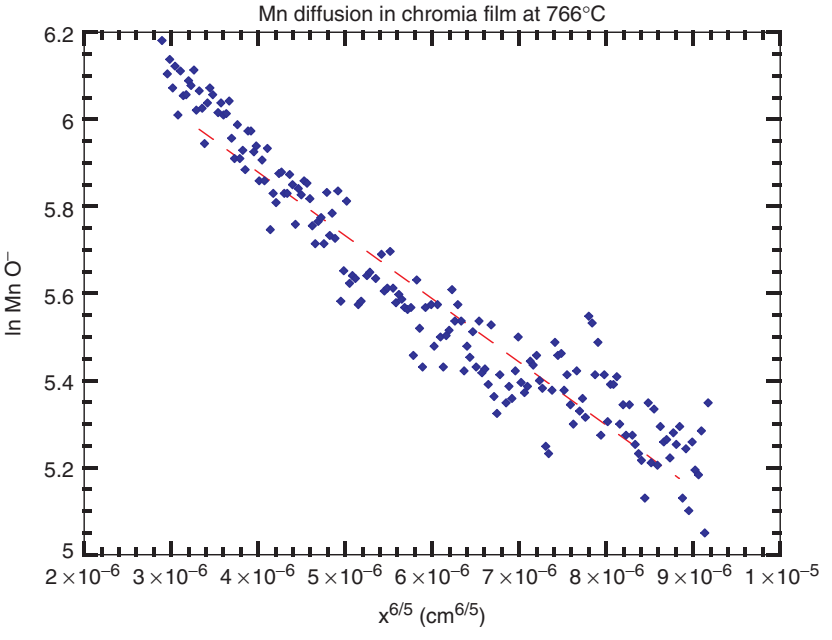

Figure 4. Penetration profile vs. $x^{6/5}$, corresponding to grain boundary diffusion, for MnO^- ion after the diffusion treatment at 766°C in a chromia film (same experiment than in figure 3).

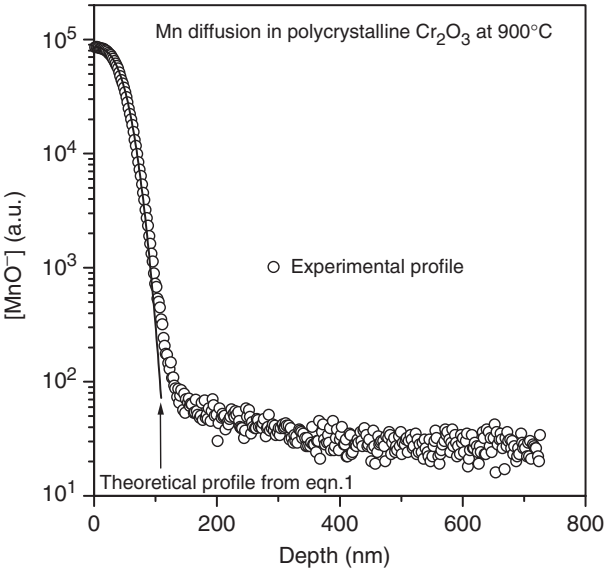

Figure 5. Penetration profile of manganese vs. x obtained in a chromia polycrystal after diffusion at 900°C. The slope of the straight line corresponds to the theoretical diffusion profile given by equation (1) for bulk diffusion.

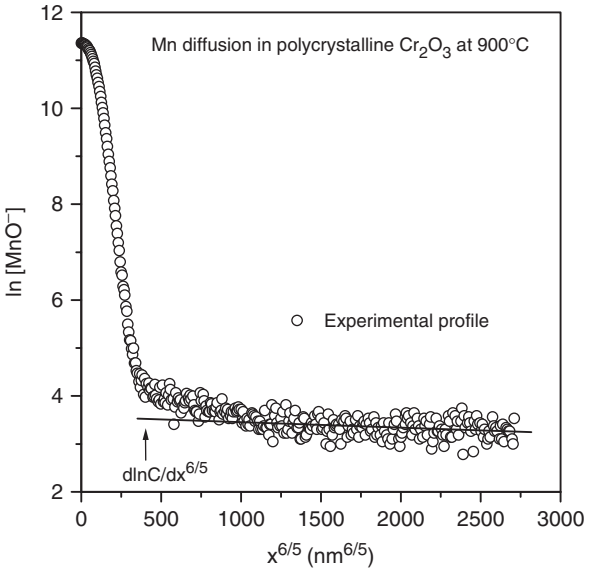

Figure 6. Penetration profile of manganese vs. $x^{6/5}$, corresponding to grain boundary diffusion, after the diffusion treatment at 900°C in a chromia polycrystal (same experiment than in figure 5). The slope of the straight line corresponds to the gradient $\partial \ln C/\partial x^{6/5}$.

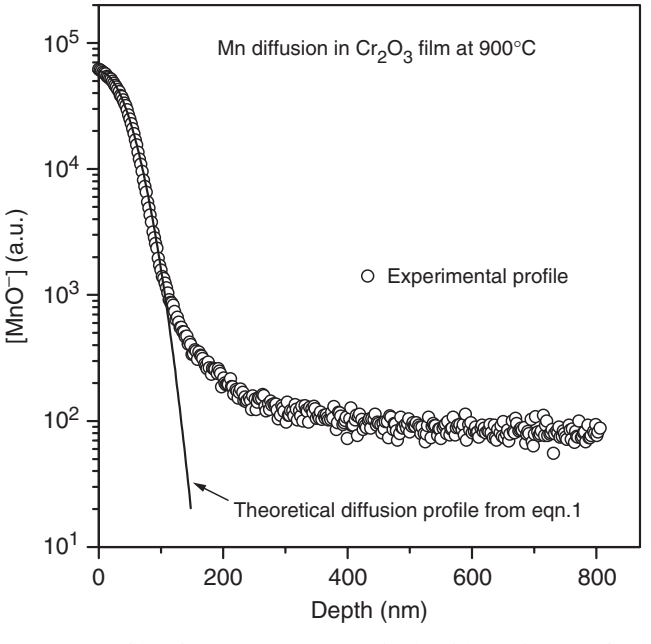

Figure 7. Penetration profile of manganese vs. x obtained in a chromia film after diffusion at 900°C. The slope of the straight line corresponds to the theoretical diffusion profile given by equation (1) for bulk diffusion.

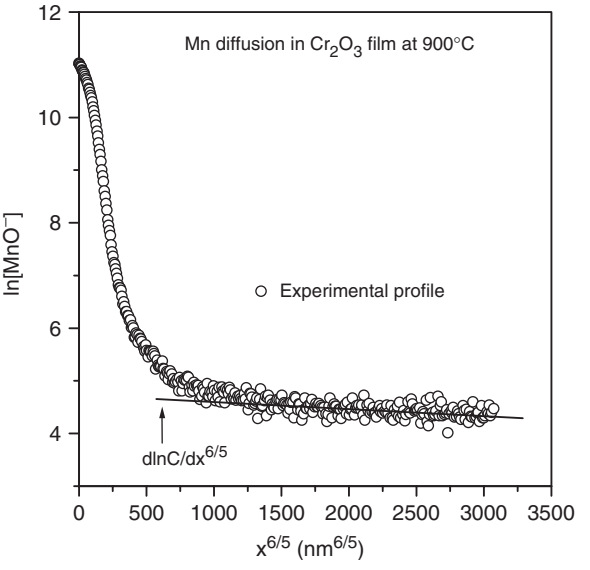

Figure 8. Penetration profile of manganese vs. $x^{6/5}$, corresponding to grain boundary diffusion in a chromia film, after the diffusion treatment at 900°C (same experiment than in figure 7). The slope of the straight line corresponds to the gradient $\partial \ln C/\partial x^{6/5}$.

Table 1. Manganese diffusion in polycrystalline Cr_2O_3.

T (°C)	pO_2 (atm)	t (s)	D_b (cm^2 s^{-1})	αD_{gb} (cm^2 s^{-1})
900	10^{-4}	5.79×10^4	3.55×10^{-17}	1.3×10^{-11}
900	10^{-4}	5.79×10^4	3.48×10^{-17}	9.71×10^{-12}
1000	10^{-4}	1.62×10^4	1.87×10^{-16}	1.65×10^{-11}
1100	10^{-4}	3.9×10^3	9.76×10^{-16}	1.56×10^{-10}
1100	10^{-4}	3.9×10^3	1.16×10^{-15}	1.38×10^{-10}

Table 2. Manganese diffusion in Cr_2O_3 films formed on $Ni_{70}Cr_{30}$ alloy.

T (°C)	pO_2 (atm)	t (s)	D_b (cm^2 s^{-1})	αD_{gb} (cm^2 s^{-1})
700	10^{-4}	1.45×10^5	6.23×10^{-18}	1.53×10^{-13}
700	10^{-4}	1.45×10^5	5.96×10^{-18}	2.88×10^{-13}
766	10^{-4}	5.76×10^4	1.93×10^{-17}	6.55×10^{-13}
766	10^{-4}	5.76×10^4	3.30×10^{-17}	1.11×10^{-12}
832	10^{-4}	4.02×10^4	5.85×10^{-17}	2.90×10^{-12}
832	10^{-4}	4.02×10^4	5.73×10^{-17}	3.01×10^{-12}
900	10^{-4}	1.47×10^4	2.08×10^{-16}	4.71×10^{-11}
900	10^{-4}	1.47×10^4	3.07×10^{-16}	2.58×10^{-11}

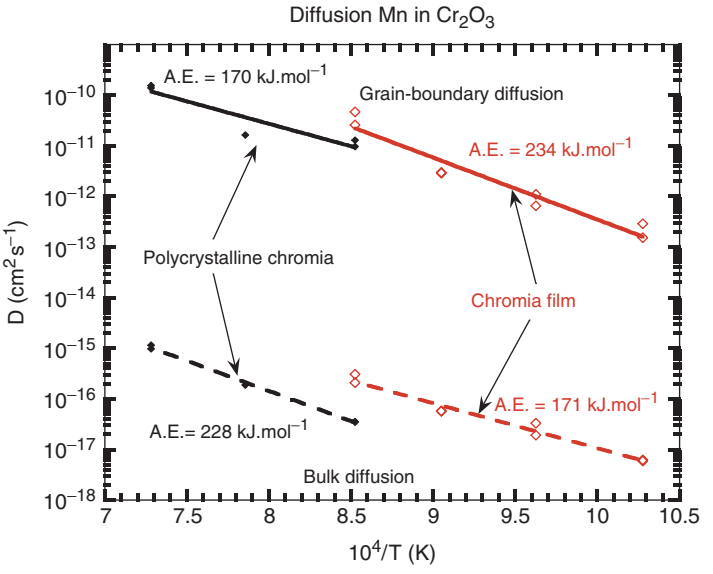

Figure 9. Arrhenius plot of bulk and grain boundary diffusion of manganese in chromia polycrystals and films.

Table 3. Arrhenius equations for bulk and grain boundary diffusion of Mn in Cr_2O_3.

Chromia polycrystal	Chromia film
$D_b(\text{cm}^2\,\text{s}^{-1}) = 4.8 \times 10^{-7} \exp\left[-\frac{228 \pm 50}{RT}\right]$	$D_b(\text{cm}^2\,\text{s}^{-1}) = 8.7 \times 10^{-9} \exp\left[-\frac{171 \pm 40}{RT}\right]$
$\alpha D_{gb}(\text{cm}^2\,\text{s}^{-1}) = 3.4 \times 10^{-4} \exp\left[-\frac{170 \pm 20}{RT}\right]$	$\alpha D_{gb}(\text{cm}^2\,\text{s}^{-1}) = 0.6 \exp\left[-\frac{234 \pm 8}{RT}\right]$

4. Discussion

4.1. *Difference between manganese diffusion in polycrystals and in chromia films formed on NiCr alloys by oxidation*

Figure 9 shows that diffusion in chromia does not really differ according to the nature of chromia, i.e. in chromia as a film or as a bulk polycrystalline material, both for bulk diffusion and grain-boundary diffusion.

Concerning bulk diffusion, bulk diffusion coefficients could depend on the microstructure if the chromia films are textured or have grown in a particular direction. It does not seem to be the case for chromia films as the grains look like equiaxed grains, as shown in figure 1. Nevertheless, there is no particular reason that the amount of point defects in films and in bulk materials is similar, the more so as the oxide film is subjected to an oxygen pressure gradient and consequently to a point defect gradient. This pressure gradient is probably at the origin of the little

difference in the bulk diffusion coefficients which are somewhat greater in films than in polycrystals. Tsaï *et al.* [9], in their study of chromium and oxygen diffusion in chromia films which were slowly cooled after their growth, found bulk diffusion coefficients similar to those obtained in massive polycrystals. However, these authors considered a modified f value in the case of films, taking into account the particular roughness of the oxide films. In our case, it is not necessary, as already shown in the study of iron diffusion in chromia films and polycrystals [5], probably because the substrate was carefully polished before oxidation.

Concerning grain-boundary diffusion, it is important to remember that the penetration curve analyses lead to $\alpha D_{gb}\delta$, i.e. to the product of the grain-boundary diffusion coefficient, the boundary width (δ) and the segregation factor α. Conventionally, δ is taken as equal to 10^{-7} cm [7], and the segregation factor is unknown and should vary according to temperature and especially according to the impurities that are incorporated in the oxide. Particularly, in the case of films, it should depend on the substrate nature and purity. Consequently, it is rather surprising to obtain close $\alpha D_{gb}\delta$ values for films and polycrystals. Note, however, that it is possible that the agreement occurs only for the studied temperature range. Such close values were also obtained for iron diffusion in the same materials [5].

Nevertheless, a slight difference is obtained for the activation energy of bulk or grain-boundary diffusion according to the nature of chromia. Indeed, the activation energy values are as follows (see table 3 and figure 9).

For the polycrystals:

$$D_b(\mathrm{cm^2\,s^{-1}}) = 4.8 \times 10^{-7} \exp\left[-\frac{228 \pm 50}{RT}\right]$$

and

$$\alpha D_{gb}(\mathrm{cm^2\,s^{-1}}) = 3.4 \times 10^{-4} \exp\left[-\frac{170 \pm 20}{RT}\right].$$

For the chromia films:

$$D_b(\mathrm{cm^2\,s^{-1}}) = 8.7 \times 10^{-9} \exp\left[-\frac{171 \pm 40}{RT}\right]$$

and

$$\alpha D_{gb}(\mathrm{cm^2\,s^{-1}}) = 0.6 \exp\left[-\frac{234 \pm 8}{RT}\right].$$

It is clear that the diffusion activation energy values are obtained with a great uncertainty, the more so as the number of experimental values are limited, especially for polycrystals and the difference, about 50 kJ mol^{-1}, between films and polycrystals is perhaps not significant. It suggests that the diffusion mechanism is similar for both materials. Nevertheless, it can be considered as surprising to obtain, in the case of films, an activation energy for grain boundary diffusion (234 kJ mol^{-1}) greater than the activation energy for bulk diffusion (171 kJ mol^{-1}). Such observations are

frequent in oxides [3, 5, 9–11], probably due to segregation phenomena or the presence of impurities along grain boundaries.

4.2. *Comparison with Cr and Fe diffusion in polycrystalline Cr_2O_3*

Figure 10 allows the comparison of results obtained in chromia polycrystals for chromium diffusion [4, 9, 12], for iron diffusion [5] and for the manganese diffusion characterized in this study. Data obtained by other authors are given in table 4.

In the bulk, clearly there is no difference; the three cations diffuse at the same rate. This is somewhat surprising since Mn^{2+} ions are larger (0.080 nm) than both Cr^{3+} (0.062 nm) and Fe^{3+} (0.065 nm) ions.

Along grain boundaries, in the studied temperature range, it could be considered that the differences are slight. Nevertheless, if this seems reasonable for the diffusion of chromium and manganese, although manganese diffusion looks like somewhat faster, it is not the case for iron diffusion. Indeed, it clearly appears that the activation energy for grain-boundary diffusion of iron (347 kJ mol^{-1}) is much greater than that for grain-boundary diffusion of chromium (135 kJ mol^{-1}) and manganese (170 kJ mol^{-1}), and at lower temperatures iron diffusion will be slower than manganese or chromium diffusion. This difference could be related to the possible diffusion of iron as Fe^{2+} interstitials, as suggested sometimes in the case of iron diffusion in Fe_2O_3 [14], as its ionic radius is then greater (0.076 nm). Nevertheless, it seems less probable in the case of Cr_2O_3 since this oxide is not deficient in oxygen as is Fe_2O_3. The discussion on the reasons for the differences between the activation

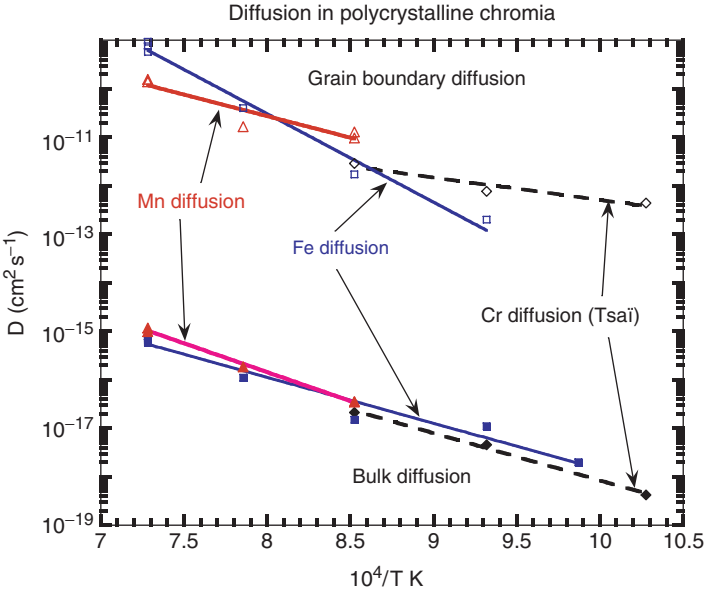

Figure 10. Comparison, in an Arrhenius plot, of bulk and grain boundary diffusion of cations in chromia polycrystals.

Table 4. Diffusion data for Cr diffusion and Fe diffusion [5].

			Chromia polycrystals		Chromia films	
Diffusion coefficients ($cm^2 s^{-1}$)	T (°C)	pO_2 (atm)	D_b ($cm^2 s^{-1}$)	αD_{gb} ($cm^2 s^{-1}$)	D_b ($cm^2 s^{-1}$)	αD_{gb} ($cm^2 s^{-1}$)
Cr diffusion (Tsaï [4, 9, 12])	700	0.1	4.2×10^{-19}	4.4×10^{-13}	2.9×10^{-18}	5.1×10^{-13}
	800	0.1	4.6×10^{-18}	7.7×10^{-13}	5.9×10^{-18}	1.1×10^{-12}
	900	0.1	2.1×10^{-17}	2.9×10^{-12}	2.0×10^{-17}	9.3×10^{-12}
Cr diffusion (Löbnig [13])	900	10^{-15}			7×10^{-15}	2×10^{-10}
					8×10^{-16}	5×10^{-11}
	740	10^{-4}	3.5×10^{-18}	5.9×10^{-12}		
	800	10^{-4}	1.1×10^{-17}	8.0×10^{-12}		
	900	7.20×10^{4}	1.3×10^{-17}	1.7×10^{-12}		
Fe diffusion (Sabioni *et al.* [5])	1000	1 or 10^{-4}	1.0×10^{-16}	4.0×10^{-11}		
	1100	10^{-4}	6.6×10^{-16}	7.5×10^{-10}		
	720	10^{-4}			1.2×10^{-19}	3.1×10^{-14}
	800	10^{-4}			1.7×10^{-18}	2.5×10^{-13}
	900	10^{-4}			1.0×10^{-17}	3.0×10^{-12}

energies of grain-boundary cation self-diffusion and iron or manganese heterodiffusion is hazardous on account of the limited temperature range studied for the various materials and the uncertainty on activation energy values already mentioned.

Note only, on the basis of results gathered in figure 10 for grain-boundary diffusion, that the greater the temperature, the greater the diffusion of iron when compared to chromium or manganese diffusion, and that manganese diffusion is slightly greater than cationic self-diffusion.

4.3. *Comparison with Cr and Fe diffusion in Cr_2O_3 films*

The comparison of results obtained in chromia films for chromium diffusion [4, 9, 12], for iron diffusion [5] and for manganese diffusion characterized in this study is given in figure 11 (see also the data obtained by other authors in table 4). In the bulk, as along grain boundaries, iron diffusion is slower than cationic self-diffusion, which would suggest diffusion of interstitial Fe^{2+} [14]. Whereas manganese is the fastest diffusing species in the bulk, the differences between cationic self-diffusion and Mn diffusion along grain boundaries is small, in the temperature range of this study.

Comparison with data obtained by Löbnig *et al.* [13] (see table 4 and figure 11) for chromium diffusion in chromia films indicates, as already suggested [4], that this author determined effective diffusion coefficients, partly taking into account grain-boundary diffusion, rather than bulk diffusion coefficients. Indeed the values given by these authors for bulk diffusion are greater than ours, being between our bulk and grain-boundary diffusion coefficients.

All these results are important to understand the barrier effect of chromia scales and why, during oxidation of stainless steel, manganese-rich mixed oxides are found

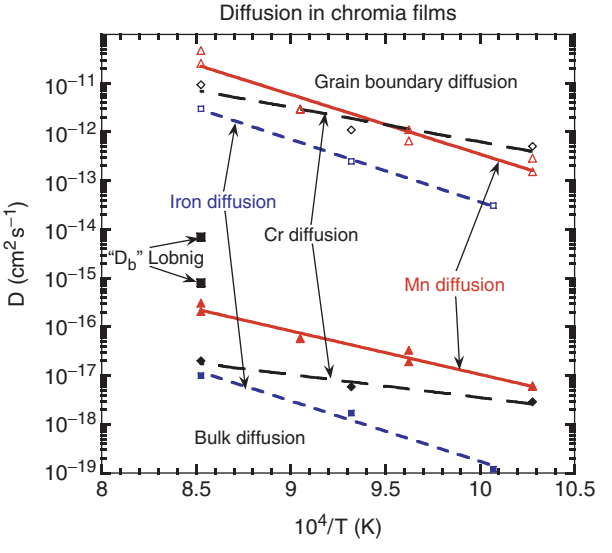

Figure 11. Comparison, in an Arrhenius plot, of bulk and grain boundary diffusion of cations in chromia films.

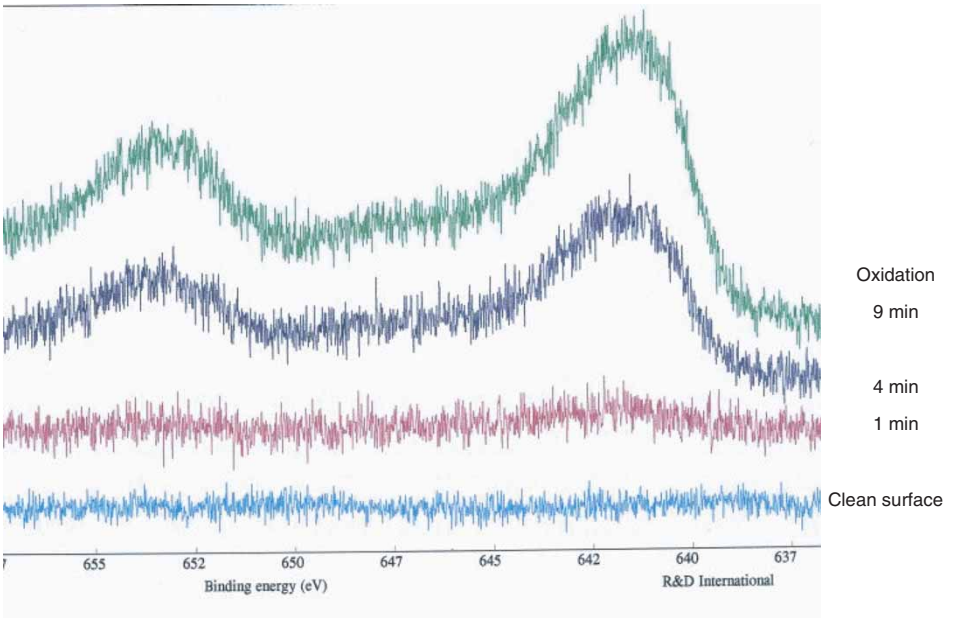

Figure 12. Mn XPS peaks obtained in a chromium steel during in situ oxidation at 600°C.

on the outer surface of the chromia films. It is well-known that chromia films act as an efficient barrier for materials used at high temperatures. For instance, in coal gasification conditions [15], carbon deposition on iron-based alloys is known to be particularly decreased by the presence of chromia film when compared to what occurs with nickel and iron oxide films. Two reasons have already been suggested and discussed previously [5] to explain the effect of chromia films, and, amongst a barrier effect and a thermodynamic one, the diffusion results suggest that the thermodynamic effect is the main parameter. Indeed, the difference between iron diffusion and chromium diffusion in chromia films is probably not sufficient to explain the spectacular differences in the carbon deposition phenomenon. Now, it is interesting to determine the mechanism by which manganese is always found on the outer surfaces of the oxide layers as mixed oxides, when oxidizing stainless steels. It is well-known that chromia films are mainly growing by grain-boundary diffusion [16]. Moreover, Tsaï showed that chromia film growth is ensured by countercurrent diffusion of anion and cation [9, 12]. Due to the fact that manganese grain-boundary diffusion is of the same order of magnitude as grain-boundary diffusion of chromium, it indicates that manganese oxide is formed at the beginning of oxidation at the same time than chromia particles, which agrees the fact that manganese affinity for oxygen is slightly greater than chromium affinity. This assumption is corroborated by figure 12, which shows that the presence of manganese on the chromia film is observed at the beginning of oxidation [15]. Then, during further oxidation, manganese ions diffuse, as do chromium ions, through chromia towards the outer surface of the film, but the amount of manganese oxide on the top of the film is limited by the small amount of manganese in the steel, compared to chromium. Afterwards, MnO particles react with chromium ions to give a spinel oxide.

5. Conclusion

Manganese diffusion in chromia was studied in both polycrystals and oxide films formed by oxidation of Ni–30Cr alloy in the temperature range 700–1100°C at an oxygen pressure equal to 10^{-4} atm. Using SIMS to establish the penetration profiles, both bulk (D_b) diffusion coefficients and grain-boundary diffusion ($\alpha D_{gb}\delta$) parameters were determined for polycrystals and films.

Manganese diffusion does not really differ according to the formation process of chromia, i.e. as a polycrystal or as a thin film formed by oxidation: both bulk and grain-boundary diffusion coefficients in chromia films and in chromia polycrystals are of the same order of magnitude. The activation energy for grain-boundary diffusion in films is greater than the activation energy determined for bulk diffusion in the same chromia films. Such results were previously observed with other oxides and are probably associated with segregation phenomena along grain boundaries, as the grain-boundary parameter determined by diffusion studies corresponds to αD_{gb}, α being a segregation factor.

In polycrystalline chromia, there is no difference between manganese, iron and chromium bulk diffusion. However, along grain boundaries, even if there are no fundamental differences in the studied temperature range, it clearly appears that the activation energy of iron is greater than activation energy of manganese and chromium leading to a slower grain-boundary diffusion of iron at lower temperatures ($T \leq 800$°C). It seems that manganese grain-boundary diffusion is slightly faster than chromium grain-boundary diffusion.

In chromia films, iron diffusion is the slowest in both the bulk and along grain boundaries. Manganese diffuses slightly faster than chromium in the bulk, but along grain boundaries, the difference is not significant.

These results indicate that the barrier effect provided by chromia against the diffusion of other elements when used as a protective coating for high temperature materials is not only due to a diffusion effect. Even if it acts as a diffusion barrier when compared to nickel or iron oxides, it also decreases the oxygen potential at the inner interface of the chromia film and prevents other metallic elements from oxidizing. But, for elements whose affinity for oxygen is at least equal to that of chromium, such as manganese, the results obtained here indicate that manganese oxide is formed at the beginning of oxidation. Then, manganese ions diffuses as chromium ions through chromia towards the outer surface of the film and, afterwards, MnO particles can react with chromium ions to give a spinel oxide.

References

[1] P. Kofstad, *High Temperature Corrosion* (Elsevier Applied Science, 1988).
[2] V. Mousseaux, PhD thesis, Le coke dansles installations de déshydrogénation de l'isobutane: formation et inhibition. University Paris VI (1994).
[3] A.C.S. Sabioni, A.M. Huntz, J. Philibert, *et al*., J. Mater. Sci. **27** 4782 (1992).
[4] S.C. Tsaï, A.M. Huntz and C. Dolin, Mater. Sci. Engng A **212** 6 (1996).
[5] A.C.S. Sabioni, A.M. Huntz, F. Silva, *et al*., Mater. Sci. Engng A **392** 254 (2005).

[6] A.C.S. Sabioni, A.M. Huntz, E.C. Luz, *et al*., Mater. Res. **6** 179 (2003).
[7] J. Philibert, *Atom Movements, Diffusion, and Mass Transport in Solids* (Les Editions de Physique, Les Ulis, 1991).
[8] A.D. Le Claire, Br. J. Appl. Phys. **14** 351 (1963).
[9] S.C. Tsaï, A.M. Huntz and C. Dolin, Oxidat. Metals **43** 581 (1995).
[10] M. Le Gall, A.M. Huntz, B. Lesage, *et al*., Phil. Mag. A **73** 919 (1996).
[11] D. Prot, M. Le Gall, B. Lesage, *et al*., Phil. Mag. A **73** 935 (1996).
[12] S.C. Tsaï, PhD thesis, University Paris-XI, Orsay (1996).
[13] R.E. Lobnig, H.P. Schmidt, K. Hennessen, *et al*., Oxidat. Metals **37** 81 (1992).
[14] K. Hoshino and N.L. Peterson, J. Phys. Chem. Sol. **46** 1247 (1985).
[15] A.M. Huntz, V. Bague, G. Beauplé, *et al*., Appl. Surf. Sci. **207** 255 (2003).
[16] A.M. Huntz, J. Phys., Paris, III **5** 1729 (1995).